# Magnetic Molecular Conductors Based on Bis(ethylenedithio)tetrathiafulvalene (BEDT-TTF) and the Tris(chlorocyananilato)ferrate(III) Complex

Suchithra Ashoka Sahadevan, Alexandre Abhervé, Noemi Monni, Pascale Auban-Senzier, Joan Cano, Francesc Lloret, Miguel Julve, Hengbo Cui, Reizo Kato, Enric Canadell, et al.

# Magnetic Molecular Conductors Based on Bis(ethylenedithio)tetrathiafulvalene (BEDT-TTF) and the Tris(chlorocyananilato)ferrate(III) Complex

Suchithra Ashoka Sahadevan,[†,‡] Alexandre Abhervé,[‡] Noemi Monni,[†] Pascale Auban-Senzier,[‖] Joan Cano,[◊] Francisco Lloret,[◊] Miguel Julve,[◊] Hengbo Cui,[#] Reizo Kato,[#] Enric Canadell,[⊥] Maria Laura Mercuri,[†,*] and Narcis Avarvari,[‡,*]

[‡]MOLTECH-Anjou, UMR 6200, CNRS, UNIV Angers, 2 bd Lavoisier, 49045 ANGERS Cedex, France

[†]Dipartimento di Scienze Chimiche e Geologiche, Università degli Studi di Cagliari, S.S. 554 − Bivio per Sestu − I09042 Monserrato (Cagliari), Italy

[‖]Laboratoire de Physique des Solides, UMR 8502, Bât. 510, CNRS-Université Paris-Sud, 91405 Orsay, France

[◊]Departament de Química Inorgànica, Instituto de Ciencia Molecular (ICMOL), Universitat de València, Paterna 46980, València, Spain

[#]Condensed Molecular Materials Laboratory, RIKEN, 2-1 Hirosawa, Wako, Saitama 351-0198, Japan

[⊥]Institut de Ciència de Materials de Barcelona (CSIC), Campus de la UAB, E-08193, Bellaterra, Spain

**ABSTRACT**

Electrocrystallization of the BEDT-TTF organic donor in the presence of the $[Fe(ClCNAn)_3]^{3-}$ tris(chlorocyananilato)ferrate(III) paramagnetic anion in different stoichiometric ratios and solvent mixtures afforded two different hybrid systems formulated as $[BEDT\text{-}TTF]_4[Fe(ClCNAn)_3]\cdot 3H_2O$ (**1**) and $[BEDT\text{-}TTF]_5[Fe(ClCNAn)_3]_2\cdot 2CH_3CN$ (**2**). Compounds **1** and **2** present unusual

structures without the typical segregated organic and inorganic layers, where layers of **1** are formed by *Λ* and *Δ* enantiomers of the anionic paramagnetic complex together with mixed-valence BEDT-TTF tetramers, while layers of **2** are formed by *Λ* and *Δ* enantiomers of the paramagnetic complex together with dicationic BEDT-TTF dimers and monomers. Compounds **1** and **2** show semiconducting behaviors with room temperature conductivities of ca. 6 x $10^{-3}$ S $cm^{-1}$ (ambient pressure) and $10^{-3}$ S $cm^{-1}$ (under applied pressure of 12.1 GPa) respectively, due to strong dimerization between the donors. Magnetic measurements performed on compound **1** indicate weak antiferromagnetic coupling between high-spin $Fe^{III}$ ($S_{Fe}$ = 5/2) and mixed-valence radical cation diyads $(BEDT\text{-}TTF)_2^{+\bullet}$ ($S_{rad}$ = ½) mediated by the anilate ligands, together with an important Pauli paramagnetism typical for conducting systems.

## 1. INTRODUCTION

Magnetic molecular conductors are a challenging class of multifunctional materials of special interest in contemporary material science, since coexistence or even interplay between delocalized π-electrons and localized d-electrons can lead to unusual and peculiar phenomena such as magnetic field-induced superconductors, magnetoresistance effects, magnetic field- switchable conductors *etc.*, with technological applications in molecular electronics and spintronics.[1] Molecular π–d systems exhibit a variety of types of electron transport (conducting, semiconducting and insulating) which can be finely tuned by the π–d interactions and, therefore, by a wise choice of both the organic donor, carrier of conductivity, and magnetic counter ions, carriers of magnetic properties (ferro-, ferri-, antiferromagnetism). Among the organic donors, the BEDT-TTF molecule,[1d-e,2] along with its selenium derivatives, is the most successful donor which has produced the majority of known superconductors and several charge-transfer salts showing different conducting states (conducting, semiconducting, *etc.*). Tetrahedral and octahedral mononuclear complexes, such as $[MX_4]^{n-}$ ($M = Fe^{III}, Cu^{II}$; X = Cl, Br)[3] and $[M(ox)_3]^{3-}$ (ox = oxalate),[1e,4] respectively, have been reported as the most relevant charge-compensating magnetic anions used to construct magnetic molecular conductors; another important milestone has been achieved by using bimetallic oxalate-based layers of the type $[M^{II}M^{III}(ox)_3]^-$ ($M^{II}$ = Mn, Co, Ni, Fe, Cu; $M^{III}$ = Fe, Cr),[5] showing a peculiar honeycomb packing pattern. Recently metal-complexes containing derivatives of the 2,5- dihydroxy-1,4-benzoquinone-3,6- disubstituted, hereafter called

anilates, have been prepared by some of us and studied extensively,[6] because they have a delocalized moiety that can mediate magnetic interactions between metal centers coordinated to the ligand. Moreover these ligands, being redox-active, can form organic radicals which should lead to strong spin coupling with paramagnetic species. Anilato-based metal complexes are also versatile building blocks for constructing functional and multifunctional luminescent[7] or conducting/magnetic molecule-based materials.[8-10] Recently, by combining the BEDT-TTF organic donor, carrier of conducting layers, with the tris(chloranilato)ferrate(III) $[Fe(Cl_2An)_3]^{3-}$ anionic magnetic complex,[6b] a series of magnetic molecular conductors with different donor/anion stoichiometric ratio have been obtained.[9a,9d] Furthermore, a complete series of chiral conductors with the chiral donor TM-BEDT-TTF[11] and a chloranilate-bridged heterobimetallic network was reported by Mercuri, Avarvari *et al.*[12] Since the presence of different substituents at the 3,6-positions of the anilate molecule can lead to the modulation of the π–π stacking, intermolecular halogen-bonding, hydrogen-bonding and dipolar interactions, we set out to use non-symmetric chloro-cyananilato based anionic complexes in molecular conductors where the variation of the ligand substituents should play a paramount role on the structural and physical properties of the obtained materials. Note that some of us reported on the use of the chlorocyananilato monoanion $[HClCNAn]^-$ in BEDT-TTF-based conducting radical cation salts,[10c] yet no examples containing a $[M(ClCNAn)_3]^{n-}$ anion complex have been reported to date. We describe herein two chlorocyananilate-based compounds formulated as $[BEDT\text{-}TTF]_4[Fe(ClCNAn)_3]\cdot 3H_2O$ (**1**) and $[BEDT\text{-}TTF]_5[Fe(ClCNAn)_3]_2\cdot 2CH_3CN$ (**2**) obtained by electrocrystallization, together with their in-depth crystal structures analysis and physical properties.

## 2. RESULTS AND DISCUSSIONS

**Synthesis.** The tris(chlorocyananilato)ferrate(III) complex $[PPh_4]_3[Fe(ClCNAn)_3]$[6c] and the BEDT-TTF donor were combined in electrocrystallization experiments, by using different solvents and current density (see Experimental Section). Two different hybrid systems formulated as $[BEDT\text{-}TTF]_4[Fe(ClCNAn)_3]\cdot 3H_2O$ (**1**) and $[BEDT\text{-}TTF]_5[Fe(ClCNAn)_3]_2\cdot 2CH_3CN$ (**2**) were obtained as reported in Scheme1. These systems mainly differ in the donor/anion ratio of 4:1 and 5:2 phase in **1** and **2** respectively, which, along with the different crystallization solvent molecules present in the structures, influence the crystal packing motif exhibited by the BEDT-TTF molecules and the resulting physical properties (*vide infra*).

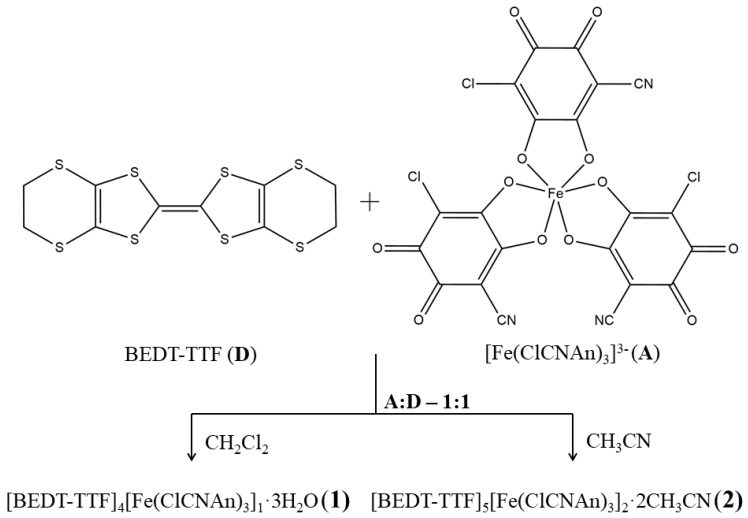


**Scheme 1**. BEDT-TTF organic donor (D), $[Fe(ClCNAn)_3]^{3-}$anionic complex (A) and experimental conditions used for the synthesis of compounds **1** and **2**.

**Crystal Structures.** The crystal structures of the two hybrid systems consist of tris-anilate anionic Fe complexes and BEDT-TTF donors with different oxidation states. As a result of the different electrocrystallization solvents used, **1** crystallized with water molecules (three per formula unit according to the SQUEEZE program), while **2** contains two acetonitrile solvent molecules in its crystal structure. In both systems the metal complexes exhibit octahedral $FeO_6$ coordination geometry, with the $Fe^{III}$ ion surrounded by three $ClCNAn^{2-}$ chelating ligands. They are therefore chiral anions, yet both *Λ* and *Δ* enantiomers are present in the crystal structures. The magnetic anions are relatively isolated as shown by the Fe···Fe distances of ca. 9.32 Å and 11.77 Å for **1** and 9.95 Å and 11.04 Å for **2** (Figure S1). In **1**, one of the anilate ligands presents a structural disorder, since the chloro and cyano substituents are equally distributed over the two positions, as usually observed in chlorocyananilate coordination polymers.[10d] The molecular structure of the anionic complex in **2** is represented in Figure 1.

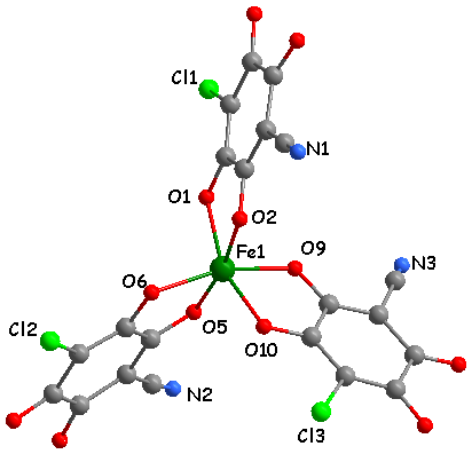


**Figure 1**. Structure of the tris(chlorocyananilato)ferrate(III) anionic complex (*Λ* enantiomer) in **2**.

The metal−oxygen bond distances in compounds **1** and **2** vary in the 1.987(4)−2.034(5) Å range (Table 1) and are similar to the distances observed in the corresponding BEDT-TTF radical cation salt with the homosubstituted chloranilate complex.[9a]

**Table 1. Fe−O Bond Distances (Å) for the Anionic Complex in Compounds 1 and 2**

| **Bonds** | **Distances (Å)** | |
|---|---|---|
| | **1** | **2** |
| Fe-O(1) | 2.022(8) | 2.006(4) |
| Fe-O(2) | 1.999(10) | 2.022(3) |
| Fe-O(5) | 1.997(10) | 2.027(3) |
| Fe-O(6) | 2.014(11) | 1.987(4) |
| Fe-O(9) | 2.022(8) | 2.034(5) |
| Fe-O(10) | 2.000(12) | 2.015(4) |
| Average | 2.009 | 2.015 |

The C−O bond distances are influenced by the coordination to the metal center. The oxygen atoms coordinated to the metal have C−O distances slightly longer than those of the peripheral oxygen atoms, which show a major double bond character.

Compound **1** crystallizes in the monoclinic space group $P2_1/c$. The asymmetric unit contains four independent BEDT-TTF donor molecules (labeled as A, B, C and D) for one $[Fe(ClCNAn)_3]^{3-}$ complex (Figure S2).

The unusual crystal packing of **1** consists of hybrid organic-inorganic layers formed by repeating units of D-A-B-C BEDT-TTF molecules along the *a* axis intercalated by $[Fe(ClCNAn)_3]^{3-}$

complexes of both chiralities as shown in Figure 2. Very short S···S contacts (3.29–3.61 Å) less than the sum of the van der Waals radii (3.65 Å) are present between the B and C molecules which form strong dimers (Figure 3).

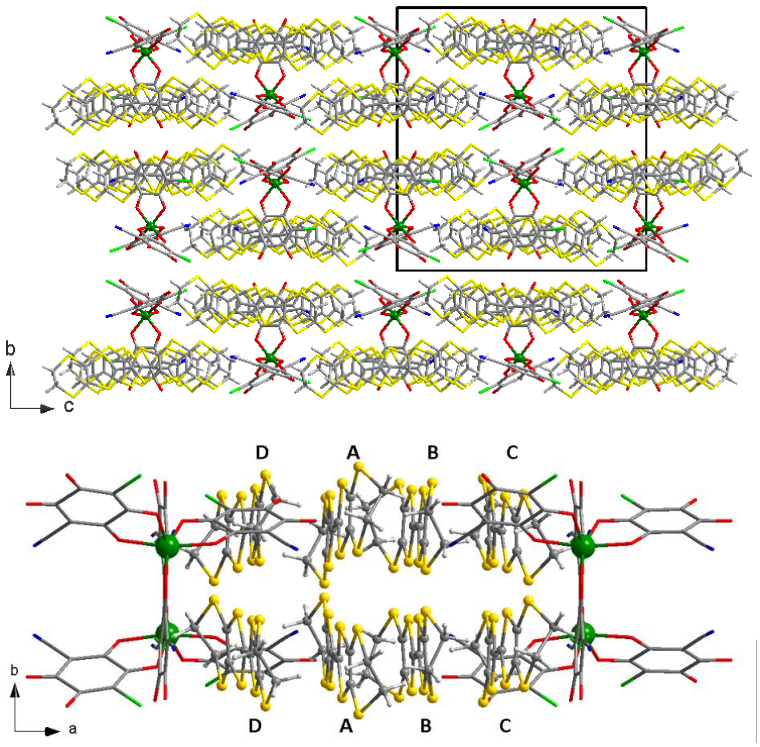


**Figure 2**. Crystal packing of **1** in the *bc* plane (top) and the *ba* plane with A, B, C and D labels (bottom). Solvent molecules are omitted for clarity.

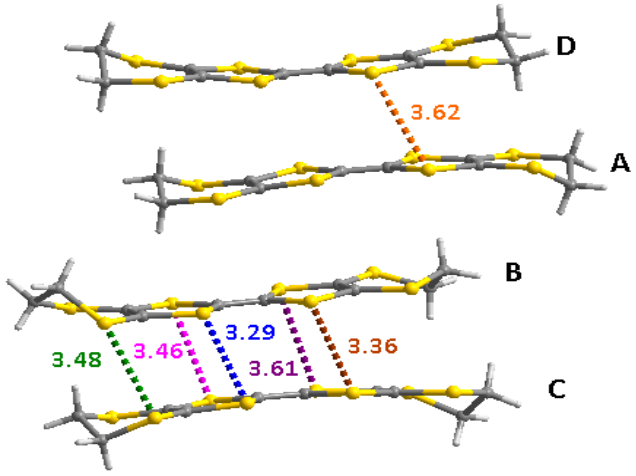


**Figure 3.** S···S interactions (Å) in **1** shorter than the sum of the van der Waals radii (3.65 Å) :S4A-S28D 3.62, S16B-S24C 3.48, S13B-S21C 3.46, S14B-S22C 3.29, S11B-S19C 3.61, S12B- S20C 3.36.

The role of the intermolecular interactions is crucial in templating this type of hybrid organic-inorganic molecular packing since the anionic complexes establish Cl···S and N···S interactions with the BEDT-TTF molecules (Figure 4).

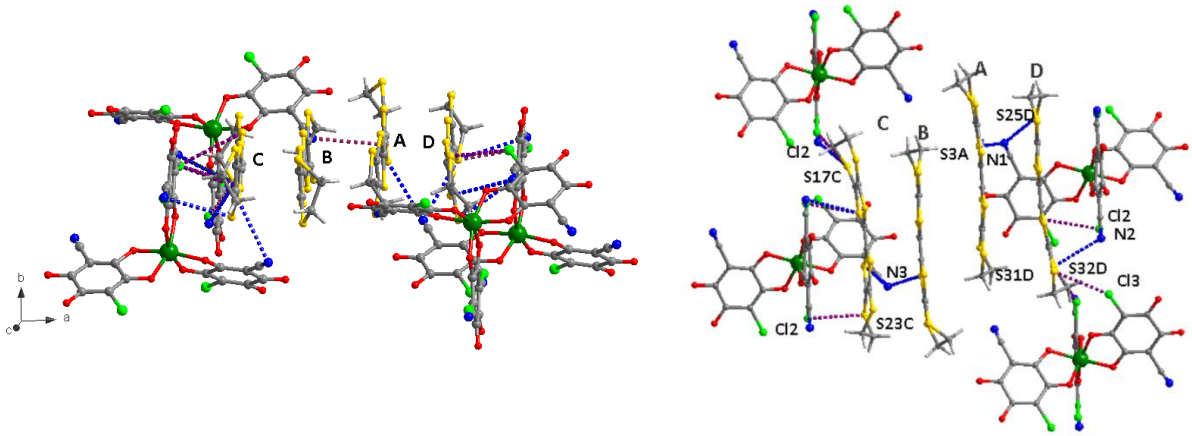


**Figure 4.** DABC BEDT-TTF molecules surrounded by metal complexes in **1**. Solvent molecules are omitted for clarity. Intermolecular Cl···S (violet) and N···S interactions (blue) lower than the sum of the van der Waals radii between the BEDT-TTF molecules and the ClCNAn ligands are highlighted (Å). Cl2-S17C 3.51, Cl2-S23C 3.60, Cl2B-S19C 3.44, Cl2-S23C 3.60, Cl2-S29D 3.50, N3-S21C 3.59, N3-S13B 3.53.

Analysis of the bond distances has been carried for each BEDT-TTF molecule following the procedure described by Day et al.[13] The results of the empirical equation Q = 6.347 − 7.463δ, relating the charge Q to the parameter δ defined by δ =(b + c) − (a + d), where a−d represent averaged values of C=C and five-membered-ring C−S bonds, are reported in Table 2. The calculated Q value of the cationic part of compound **1** is +3, as expected from the sum of the charge calculated for each of the four BEDT-TTF donor molecules present in this salt (Table 2).

**Table 2: Bond Distance Analysis and Selected Bond Distances (Å) for the BEDT-TTF Donor Molecules in 1**

| | | A | B | C | D |
|---|---|---|---|---|---|
| | a | 1.378(22) | 1.366(20) | 1.425(20) | 1.356(16) |
| | b | 1.710(16) | 1.720(14) | 1.706(14) | 1.724(11) |
| | | 1.748(15) | 1.737(14) | 1.706(14) | 1.729(11) |
| | | 1.742(14) | 1.724(13) | 1.716(13) | 1.743(11) |
| | | 1.717(14) | 1.711(13) | 1.702(13) | 1.729(11) |
| | c | 1.756(14) | 1.726(14) | 1.750(14) | 1.707(12) |
| | | 1.747(14) | 1.745(13) | 1.767(14) | 1.740(13) |
| | | 1.759(13) | 1.723(16) | 1.726(14) | 1.756(13) |

| | | | | | |
|---|---|---|---|---|---|
| 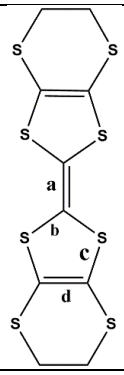 | | 1.763(13) | 1.745(14) | 1.752(13) | 1.723(11) |
| | d | 1.344(18) | 1.324(20) | 1.354(20) | 1.345(18) |
| | | 1.329(20) | 1.381(20) | 1.334(18) | 1.350(18) |
| δ=(b+c)-(a+d) | δ | 0.771 | 0.739 | 0.687 | 0.759 |
| Q= 6.347-7.4638·δ | Q | 0.59 | 0.82 | 1.21 | 0.68 |

The values of central C=C and internal C–S bond lengths confirm that B and C molecules, associated in strong dimers, bear a charge of +1, whereas D and A molecules are present in a mixed-valence state.

The BEDT-TTF molecular packing in compound **1**, along with the mixed-valence state of donorsA and D bearing 0.59 and 0.68 positive charge, respectively, are in principle favorable for delocalization of the charge, in agreement with the electron transport properties (*vide infra*).

Compound **2** crystallizes in the triclinic centrosymmetric space group *P*–1. The asymmetric unit consists of two (A and B) and half (C) independent BEDT-TTF molecules (indicated as A−C in the Figures and discussion), one $[Fe(ClCNAn)_3]^{3-}$ anionic complex and one acetonitrile solvent molecule (Figure S3), thus providing the formula $[BEDT\text{-}TTF]_5[Fe(ClCNAn)_3]_2\cdot 2CH_3CN$. The crystal packing of **2** shows a pseudo-segregation of organic and hybrid organic-inorganic layers (Figure 5).

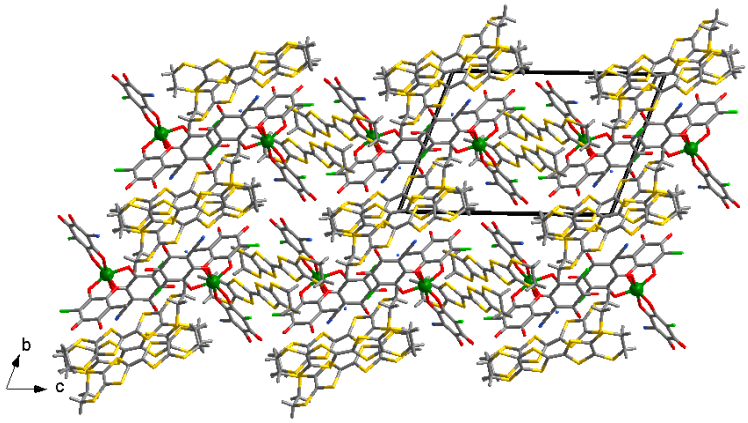


**Figure 5.** Crystal packing of **2** in *bc* plane. Solvent molecules are omitted for clarity.

The hybrid organic-inorganic layer consists of BEDT-TTF dimers (AA) surrounded by metal complexes of opposite chirality in the *bc* plane establishing Cl···S and N···S interactions (Figure 6). The organic donor layer is unusual and consists of B and C molecules arranged almost perpendicular to each other: B molecules interact in face-to-face manner forming strong dimers (BB) (Figure 7a,) while the C molecules, which are almost perpendicular to B, interact laterally. Intra- and inter-layer interactions between donor molecules are highlighted in Figures 7a-c, S4-S5.

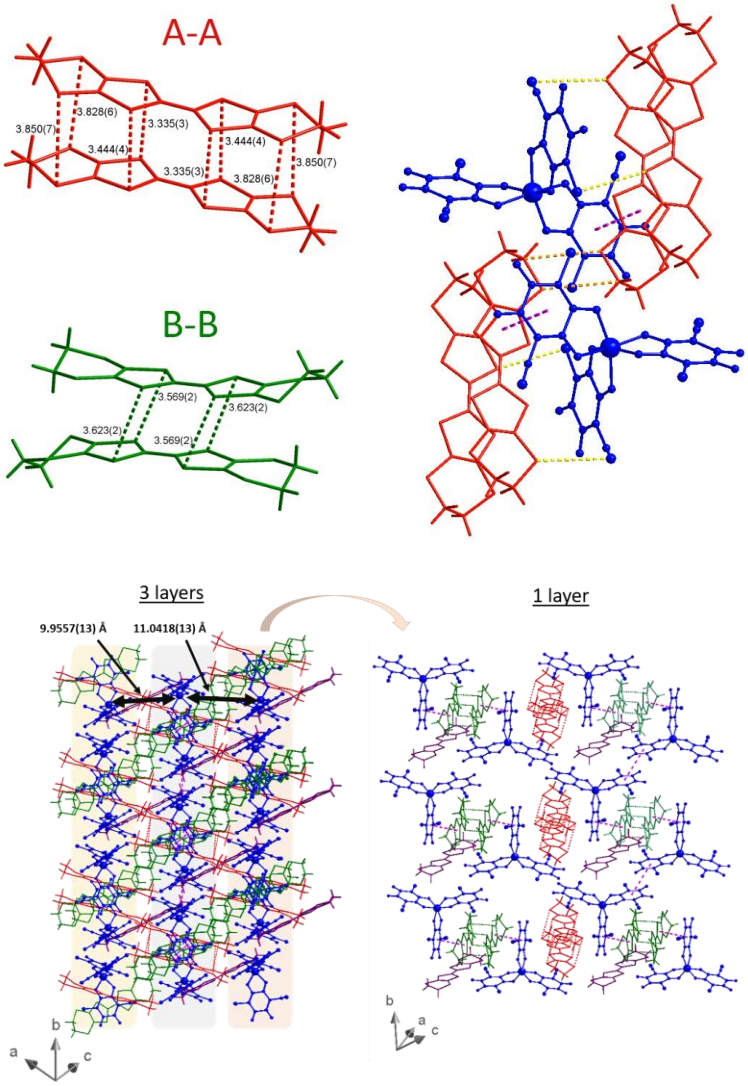


**Figure 6.** AA and BB dimers and interactions of donors with complexes in **2** (top); representation of three consecutive hybrid layers with interlayer Fe···Fe distances (bottom left) and *π*-*π* interactions in one hybrid layer (bottom right). Donor molecules A, B, C and complex are highlighted in red, green, violet and blue respectively. The dashed lines represent the intermolecular *π*-*π* interactions (pink), C-H···S interactions (orange), Cl···S and N···S interactions (yellow). C···S: 3.732(17) Å, Cl···S: 3.980(5) Å, N···S: 3.481(10) Å. Solvent molecules are omitted for clarity.

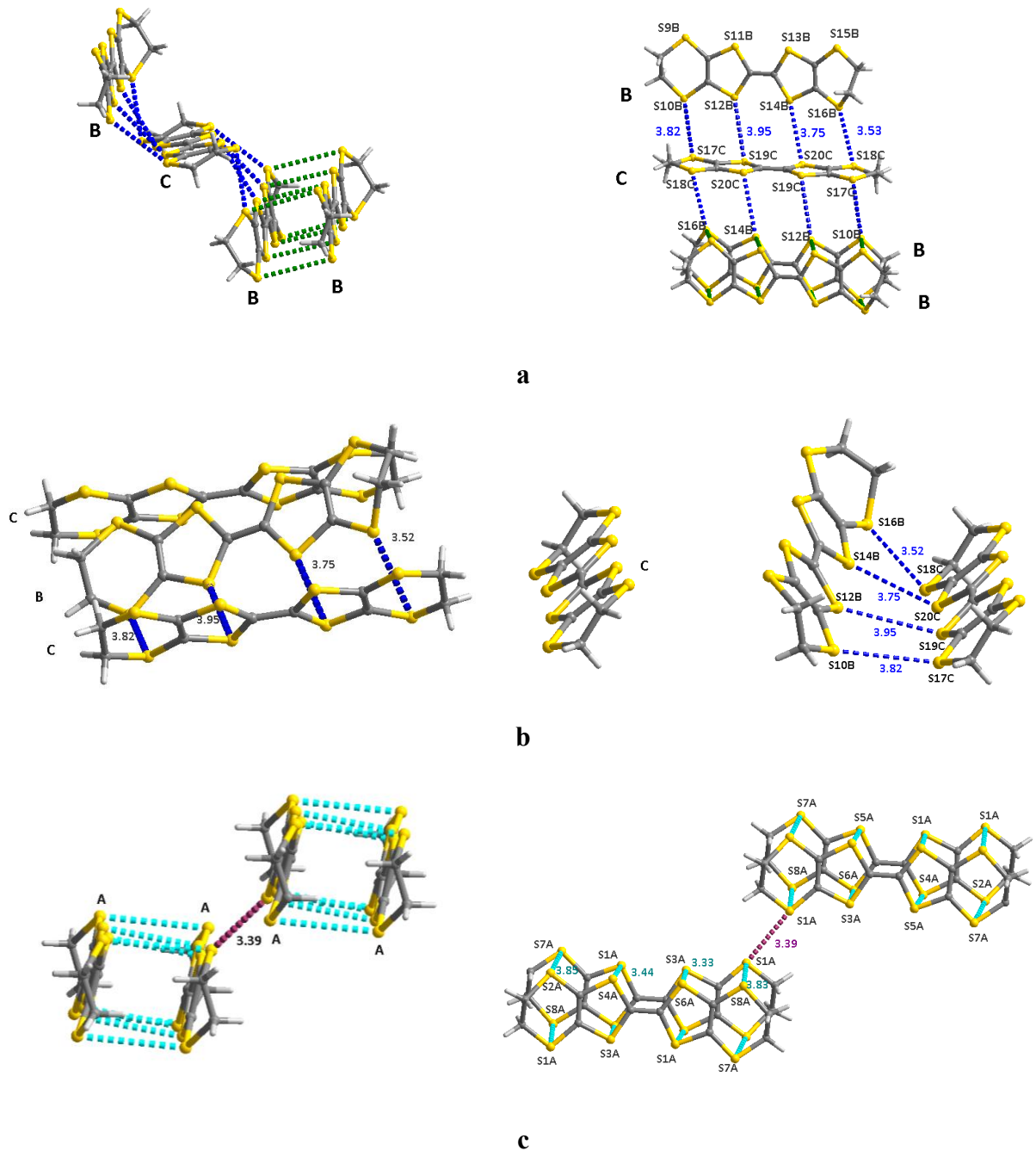


**Figure 7**. a-c) Zoom pictures highlighting the interactions in the BEDT-TTF layer in **2**. Intra- and inter-layer S···S contacts are highlighted. Face-to-face interactions are highlighted in A-A blue, B-B green; side-to-side interactions between B-C in dark blue, A-B in pink, A-A in violet, A-C in orange.

The central C=C and internal C−S bond lengths values (Table 3) confirm that the A and B molecules bear charges of +1, whereas C molecules are over-oxidised (charge +2).

**Table 3. Bond Distance Analysis and Selected Bond Distances (Å) for the BEDT-TTF Donor Molecules in 2.**

| | | A | B | C |
|---|---|---|---|---|
| 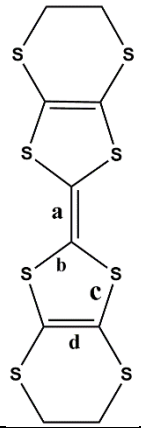 | a | 1.387(9) | 1.391(8) | 1.447(8) |
| | b | 1.709(6) | 1.721(8) | 1.695(5) |
| | | 1.720(6) | 1.717(6) | 1.680(6) |
| | | 1.701(6) | 1.714(8) | |
| | | 1.722(4) | 1.718(6) | |
| | c | 1.743(9) | 1.745(6) | 1.728(7) |
| | | 1.728(8) | 1.740(8) | 1.707(6) |
| | | 1.724(9) | 1.727(6) | |
| | | 1.728(8) | 1.734(8) | |
| | d | 1.343(1) | 1.360(1) | 1.369(8) |
| | | 1.346(1) | 1.348(1) | |
| δ=(b+c)-(a+d) | δ | 0.71 | 0.709 | 0.589 |
| Q= 6.347-7.4638·δ | Q | 1.03 | 1.05 | 1.95 |

Noteworthy, under the same experimental conditions, i.e. the BEDT-TTF organic donor, $CH_2Cl_2$ and $CH_3CN$ solvents, when the $[PPh_4]_3[Fe(Cl_2An)_3]$ salt was used instead of $[PPh_4]_3[Fe(ClCNAn)_3]$, different radical cation salts were produced with 3:1 and 5:1 ratios donor to complex,[9a] as highlighted in Table 4. It is therefore clear that intermolecular interactions such as Cl···S and N···S contacts play a paramount role in the crystal packing of compounds **1** and **2**.

**Table 4. Comparison of radical-cation salts obtained by using $[PPh_4]_3[Fe(ClCNAn)_3]$ and $[PPh_4]_3[Fe(Cl_2An)_3]$ in $CH_2Cl_2$ and $CH_3CN$ solvents.**

| Solvent | **BEDT-TTF (D)** | | | |
|---|---|---|---|---|
| | $[PPh_4]_3[Fe(ClCNAn)_3]$ (A) | | $[PPh_4]_3[Fe(Cl_2An)_3]$ (A) | |
| | this work | **D:A** | Ref. 9a | **D:A** |
| DCM | $[BEDT\text{-}TTF]_4[Fe(ClCNAn)_3]\cdot 3H_2O$ **(1)** | **4:1** | $BEDT\text{-}TTF]_3[Fe(Cl_2An)_3]\cdot 3CH_2Cl_2\cdot H_2O$ | **3:1** |
| ACN | $[BEDT\text{-}TTF]_5[Fe(ClCNAn)_3]_2\cdot 2CH_3CN$**(2)** | **5:2** | δ-$[BEDT\text{-}TTF]_5[Fe(Cl_2An)_3]\cdot 4H_2O$ | **5:1** |

**Magnetic Measurements.** The magnetic properties of **1** in the form of $\chi_M T$ versus $T$ plot [$\chi_M$ being the magnetic susceptibility per one iron(III) ion] are shown in Figure 8. At room temperature, $\chi_M T$ is 5.23 $cm^3$ $mol^{-1}$ K. Upon cooling, $\chi_M T$ exhibits a practically linear decrease until ca. 80 K and below this temperature it decreases abruptly to reach 3.0 $cm^3$ $mol^{-1}$ K at 1.9 K. This plot is as expected for a spin sextet ($S_{Fe}$ = 5/2) and a spin doublet ($S_{rad}$ = ½) with a weak antiferromagnetic coupling together with an important Pauli paramagnetism, this last accounting for the linear dependence of $\chi_M T$ in the high temperature region. The zero-field splitting of the high-spin iron(III) is expected to be very small and then, the sharp decrease observed in the low temperature range of **1** has to be attributed to a relatively weak antiferromagnetic interaction between the local spins (the metal ion and the radical).

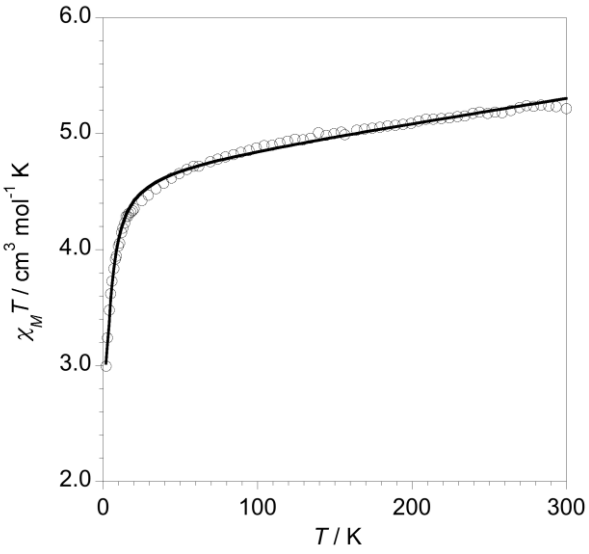


**Figure 8.** Thermal variation of the $\chi_M T$ product for 1: (o) experimental; (—) best-fit curve through eq (1) (see text).

An inspection of the crystal packing of **1** shows the occurrence of a···*DABC*Fe(III)*DABC*Fe(III)*DABC*… stacking along the crystallographic *a* axis. As the analysis of the bond distances (see above) shows that the crystallographically independent BEDT-TTF molecules bear a charge of +0.53, +0.90, +1.17 and +0.59 for *A*, *B*, *C* and *D* respectively, from a magnetic viewpoint compound **1** can be viewed as couples of a magnetically interacting spin sextet [iron(III)] and spin doublet (*DA* pair) which are connected through the diamagnetic *BC* pairs along the *a* axis. By neglecting the magnetic coupling through the diamagnetic *BC* pair, the magnetic

data of **1** were analyzed through the Hamiltonian of eq (1) which describes the magnetic interaction between a spin sextuplet ($S_{Fe}$ = 5/) and spin doublet ($S_{DA}$ = ½), an extralinear contribution corresponding to a temperature independent Pauli-like paramagnetism (TIP), typical of conducting systems being also considered:

$$\boldsymbol{H} = -J\boldsymbol{S}_{Fe}\cdot\boldsymbol{S}_{rad} + g\beta H(\boldsymbol{S}_{Fe} + \boldsymbol{S}_{rad}) \qquad (1)$$

In this expression, $J$ is the magnetic coupling and $g$ is the average Landé factor which is assumed to be identical for the iron (III) ion and the radical. Least-squares best-fit parameters are $J$ = -2.020(4) $cm^{-1}$, $g$ = 1.990(2) and TIP = 2.10(3) x $10^{-3}$ $cm^3$ $mol^{-1}$. The calculated curve (solid line in Figure 8) matches well the experimental data in the whole temperature range investigated. The weak antiferromagnetic coupling between the iron(III) an the radical from the *DC* pair which occurs in **1** is mediated by the π-π interaction involving the BEDT-TTF donor molecule and the anilate ligand of the anionic complex. As far as the value of the TIP parameter is concerned,it is of the order of those previously reported for other molecular conducting radical cation salts,[14] and in *β*'-(BEDT-TTF)$_5$[Fe($C_5O_5$)$_3$]·3$H_2O$ ($C_5O_5^{2-}$ = croconate dianion),[15] (BDH-TTP)$_6$[Fe($C_5O_5$)$_3$]·$CH_2Cl_2$[16] and (ET)$_6$[Fe($C_6O_2Cl_2$)$_3$]·3/2$H_2O$·1/2$CH_2Cl_2$ ($C_6O_4Cl_2^{2-}$ = chloranilate dianion)[9a,d] as well as in other members of the $ET_4$[($H_3O$)M(($C_2O_4$)$_3$]·S ($C_2O_4^{2-}$ = oxalate dianion and S = solvent) family.[1a,b,4d,17] Alternatively, the magnetic data can be reproduced by ruling out the magnetic interaction between the iron(III) and the *DA* pair [that is $J$ = 0 $cm^{-1}$ in eq (1)] and introducing a Weiss parameter θ as $T$-θ. In this mean-field approach, we obtain a θ value of -1.374(7) K with the same values of $g$ and TIP from the previous analysis but resulting in a poorer quality of the fit.

Unfortunately, the very small amount of compound **2** obtained precluded any accurate magnetic susceptibility measurements. However, from the analysis of the crystal structure one can infere that the donors will be essentially magnetically silent since A and B form strong dimers while C is a diamagnetic dication, therefore the magnetism should be dominated by the paramagnetism of high-spin $Fe^{III}$ (S = 5/2) ions.

**Transport Properties and Band Structure Calculations.** The conductivity measurements in compound **1** show room temperature conductivity between 2 × $10^{-4}$ and 8 × $10^{-4}$ S $cm^{-1}$. The resistivity increases as the sample is cooled down in agreement with a semiconducting behavior, $\rho = \rho_0 exp(E_a/kT)$ with an average activation energy $E_a$ of 164 meV (Figure 9, left). Compound **2**

also shows semiconducting behavior at ambient pressure with r.t. conductivity of $1.8 \times 10^{-5}$ S cm$^{-1}$ and $E_a$ of 2483 K (214 meV) (Figure 9, right). Then, temperature dependence of the resistivity under high pressure was measured only for compound **2**. The r.t. resistivity and $E_a$ decrease with pressure, while the compound shows semiconducting behavior at all measured pressures. At 12.9 GPa the room temperature conductivity was $10^{-3}$ S cm$^{-1}$ and $E_a$ 92 meV (1068 K).

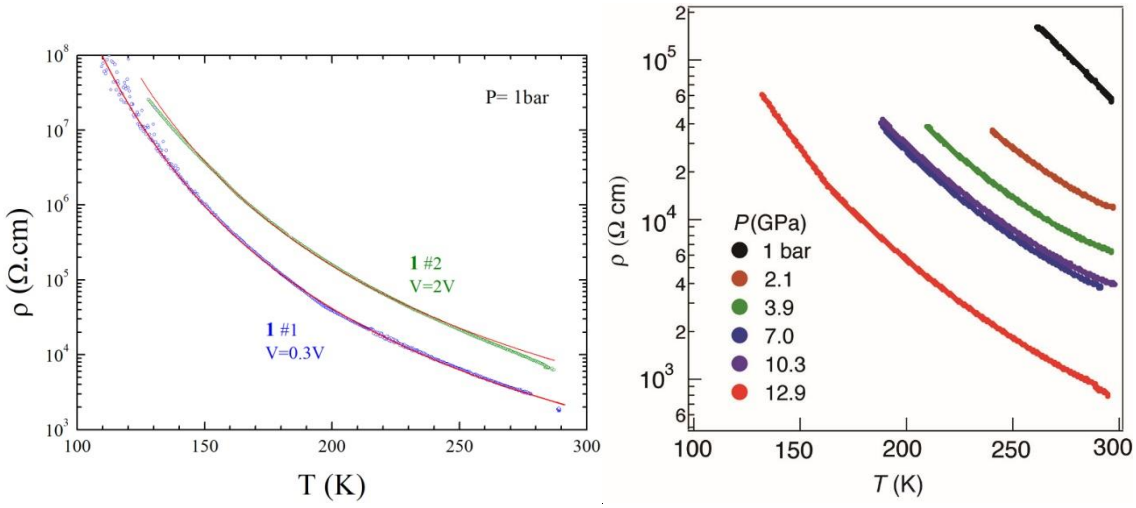


**Figure 9**. Temperature dependence of the electrical resistivity ρ for single crystals of compounds **1** at ambient pressure (left) and **2** under various pressures (right).

In order to correlate the electron transport properties with the crystal structures, tight-binding band structure calculations have been performed on both salts **1** and **2**. The repeat unit of the donor sublattice of the [BEDT-TTF]$_4$[Fe(ClCNAn)$_3$]·3H$_2$O salt **1** contains sixteen BEDT-TTF donors, i.e. four *DA* dimers and four *BC* dimers. As shown at the right of Figure 10, the HOMO splitting of the two different dimers is considerably different; that for dimer *BC* is almost twice larger, as expected from the shorter S…S contacts shown in Figure 3. The calculated band structure for the full donor sublattice of **1** is shown in Figure 10. The sixteen bands appear as four groups of four bands (because there are four dimers of each type in the repeat unit) and each group is associated with a given type of dimer as noted with different colors in Figure 10. As expected, the highest and lowest groups of bands are associated with the *BC* dimers. Taking into account the stoichiometry and the 3– charge of the anion the bands of Figure 10 must contain 12 holes. The four upper bands located on the *BC* dimers are empty and consequently these dimers must bear a 2+ charge, in agreement with the results of Table 2. According to Figure X the four remaining holes must be accommodated in the *DA* dimer levels. Although a situation where the two upper

bands are empty could be considered, this is extremely unlikely. The two pairs of bands are very flat so that the electronic repulsions will favor an electronic localization. Note that the HOMO levels splitting for the *DA* dimers is quite substantial (~ 0.6 eV). This indicates that $(DA)^+$ dimers with one hole in the antibonding combination of the two HOMOs should be quite stable whereas double occupation of this level in half of the dimers, as needed if the two lower levels are fully occupied, would be very unfavorable. In addition, a double occupation of the two lower bands would implicate the occurrence of two different types of *DA* dimers which would be at odds with the crystal structure. We thus conclude that the four *DA* levels must be singly occupied so that both donors *A* and *D* have an average +1/2 charge, in agreement with the results in Table 2.

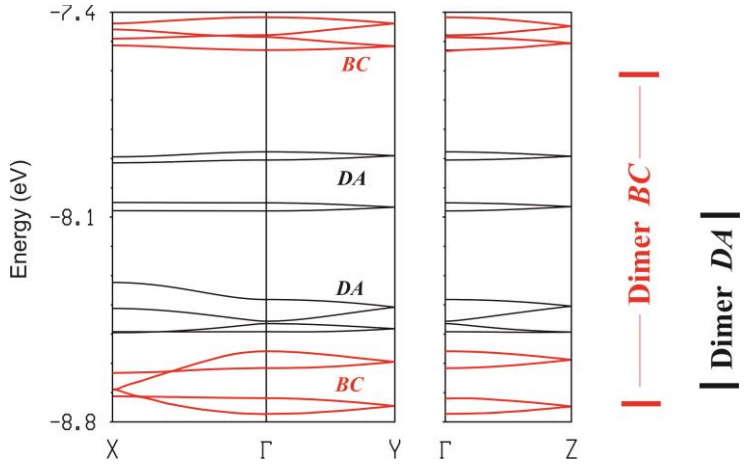


**Figure 10**. Calculated band structure for the donor lattice of $[BEDT\text{-}TTF]_4[Fe(ClCNAn)_3]\cdot 3H_2O$ where Γ = (0, 0, 0), X = (*a**/2, 0, 0), Y = (0, *b**/2, 0) and Z = (0, 0, *c**/2). The red/black bands are those localized in the *BC*/*DA* dimers, respectively. The splitting of the HOMO levels for dimers *DA* and *BC* are also indicated.

Note that (i) the four bands associated with the upper HOMO level of the *DA* dimers appear as split into two pairs, and (ii) the lower HOMO level of the *DA* dimer occurs at somewhat lower energy than the set of four bands originating from such level. This means that there are modest but non negligible interactions (i) between the pairs of *DA* dimers clearly visible in Figure 2 and (ii) between *DA* and *BC* dimers. However the bands of Figure 10 are very flat, which means that these interactions remain localized in the lattice. Consequently any interaction between the unpaired electrons of the *DA* dimers should occur through the anion. As noted above (see Figure 2) both the *DA* and *BC* dimers are very well oriented to interact with the anilate ligand of the anion so that the unpaired electrons of the anion and the *DA* dimer certainly should interact in **1**. Since the

calculations show that some *BC* character mixes into the *DA* dimer orbitals, it could well be that such interaction somewhat propagates along the *a*-direction.

The donor sublattice of the [BEDT-TTF]$_5$[Fe(ClCNAn)$_3$]$_2$·2CH$_3$CN salt **2** contains *AA* and *BB* dimers and *C* monomers. As shown at the right of Figure 11, the HOMO splitting of the two different dimers is again strong and noticeably different; that for dimer *AA* is almost twice larger due to the better orientation and shorter S···S distances. As a consequence the two levels based on the *AA* dimers lead to the upper and lowest bands of the donor sublattice of **2** (Figure 11). The upper HOMO based orbital of the BB dimer and the HOMO of the C monomer have very similar energies. Because of this fact and the short contacts between B and C donors noted in Figure 7a and b, the two orbitals interact leading to the two bands with mixed B and C character noted B+C in Figure 11. In view of the stoichiometry and the 3– charge of the anion, the bands of Figure 11 must contain 6 holes so that the three upper bands are empty. Consequently, dimers *AA* and *BB* as well as monomer *C* must have a 2+ charge, in agreement with the results of Table 3. Since there is a large band gap (~0.6 eV) separating the fully empty and filled bands the donor lattice of salt **2** must be magnetically silent.

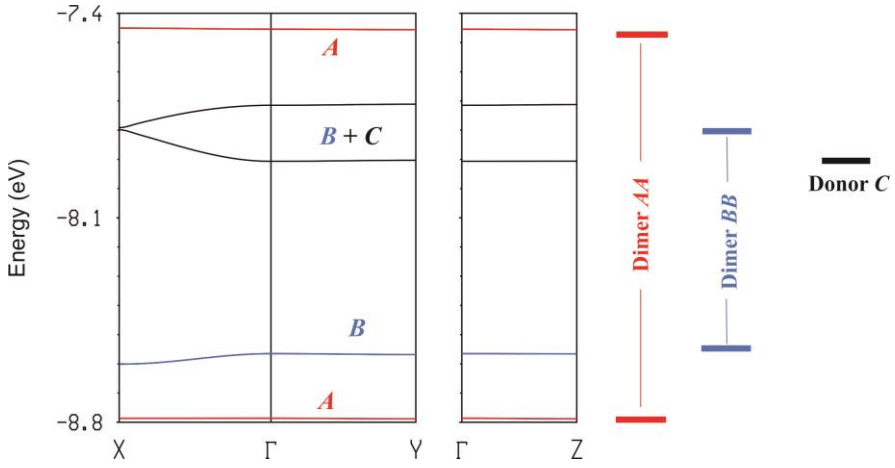


**Figure 11**. Calculated band structure for the donor lattice of [BEDT-TTF]$_5$[Fe(ClCNAn)$_3$]$_2$·2CH$_3$CN where Γ = (0, 0, 0), X = ($a$*/2, 0, 0), Y = (0, $b$*/2, 0) and Z = (0, 0, $c$*/2). The splitting of the HOMO levels for dimers *AA* and *BB* as well as the HOMO of C are also indicated.

## 3. CONCLUSIONS

Two radical cation salts based on BEDT-TTF and [Fe(ClCNAn)$_3$]$^{3-}$ tris(chlorocyanilato) ferrate(III) anionic complex have been prepared by electrocrystallization, by using $CH_2Cl_2$ for **1**

and $CH_3CN$ for **2**. In $CH_2Cl_2$, a 4:1 donor:anion salt **1** was obtained,containing mixed-valence and +1 oxidation states for the donor, while in **2**, with a 5:2 donor:anion ratio, radical cations and dicationic donors coexist. The role of Cl···S and N···S intermolecular interactions on the crystal packing of compound **1** and **2** is also highlighted. **1** and **2** compounds present unusual donor−anion segregation and both are semiconductors. Applying high pressures of up to 12.9 GPa in the case of **2** allowed to increase the conductivity by two orders of magnitude.The thermal behavior of the $\chi_M T$ product of **1** is quite interesting and corresponds to a spin sextet ($S_{Fe}$ = 5/2) and a spin doublet ($S_{rad}$ = ½) with a weak antiferromagnetic coupling together with an important Pauli paramagnetism of the order of those previously reported for other related molecular conducting radical salts.

As perspective, BEDT-TTF-based radical cation salts where the tris(chlorocyananilato)ferrate(III) anion is replaced by its Br or, in particular, I analogues at the 3,6 positions of the anilato moiety will be prepared, in order to perform a systematic study on the influence of the electronic nature and strength of the intermolecular interactions (including halogen bonding), due to the different halogen substituents, in affecting the crystal packing and, subsequently, the corresponding physical properties. The influence of electron-donating substituents in tuning the electron density of the anilato moiety will be also investigated. Of special interest would be the use of chiral donors in order to possibly select only one coordination stereochemistry around the metal center and also to combine chirality with conducting and magnetic properties.[18]

## EXPERIMENTAL SECTION

**General Considerations.** $TPPh_3[Fe(ClCNAn)_3]$ was synthesized as previously reported.[6c] BEDT-TTF (Zentek, TCI) was used as received. Electrocrystallization was performed using HPLC grade solvents (Termofisher Scientific Alfa-Aesar) previously dried under alumina and degassed with argon.

**Synthesis. $[BEDT\text{-}TTF]_4[Fe(ClCNAn)_3]\cdot 3H_2O$ (1).** Two $CH_2Cl_2$ solutions of the precursors $TPPh_3[Fe(ClCNAn)_3]$ and BEDT-TTF were prepared and respectively placed in the cathodic and anodic compartments of an H-shape electrocrystallization cell. Black blocks of single crystals of **1** were obtained on the anode electrode by appling a current density of 1 μA $cm^{-2}$ at room temperature over a period of three weeks.

**[BEDT-TTF]$_5$[Fe(ClCNAn)$_3$]$_2$·2CH$_3$CN (2)**. Black plates of single crystals of **2** were obtained in a similar experiment, by changing the $CH_2Cl_2$ solvent with $CH_3CN$ and applying a current density of 3 μA cm$^{-2}$ over a period of two months.

**X-ray Crystallography.** Data collection was performed at 150 K on an Agilent Supernova diffractometer with Cu Kα (λ = 1.54184 Å). Single crystals of **1** and **2** were mounted on a glass fiber loop using a viscous hydrocarbon oil to coat the crystal and then transferred directly to the cold nitrogen stream for data collection. The structure was solved by direct methods with the SIR97 program and refined against all F2 values with the SHELXL-97 program using the WinGX graphical user interface. All non-hydrogen atoms were refined anisotropically, and hydrogen atoms were placed in calculated positions and refined isotropically with a riding model. The program SQUEEZE from PLATON was used for **1** to determine the nature of the disordered solvent molecules. The void space of 378.8 Å$^3$ containing 127 electrons/cell indicates the presence of 3 molecules of water that have been inserted in the formula. Table 5 details the crystallographic data and structure refinement results.

**Table 5**. **Crystallographic data for compounds 1 and 2**

| | **1** | **2** |
|---|---|---|
| Empirical formula | $C_{61}H_{38}Cl_3FeN_3O_{15}S_{32}$ | $C_{48}H_{23}Cl_3FeN_4O_{12}S_{20}$ |
| Fw | 2241.06 | 1651.10 |
| Crystal color | black | black |
| Crystal size (mm3) | 0.20 * 0.10 * 0.08 | 0.20 * 0.15 * 0.10 |
| Temperature (K) | 150.00(10) | 150.00(10) |
| Wavelength (Å) | 1.54184 | 1.54184 |
| Crystal system, Z | Monoclinic, 4 | Triclinic, 2 |
| Space group | $P2_1/c$ | $P$-1 |
| a (Å) | 18.2791(10) | 13.8508(5) |
| b (Å) | 21.9785(10) | 14.5382(6) |
| c (Å) | 22.4369(11) | 18.3072(7) |
| α (°) | 90 | 67.487(4) |
| β (°) | 111.722(6) | 79.770(3) |
| γ (°) | 90 | 61.563(4) |
| V (Å$^3$) | 8373.9(7) | 2994.6(2) |
| ρcalc (g.cm$^{-3}$) | 1.778 | 1.831 |
| μ(CuKα) (mm-1) | 10.334 | 10.338 |
| θ range (°) | 2.602–72.810 | 2.613-73.623 |
| Data collected | 35680 | 23006 |
| Data unique | 16234 | 11621 |
| Data observed | 12151 | 9812 |
| Number of | 1015/58 | 811/9 |

| | | |
|---|---|---|
| parameters/restraints | | |
| R(int) | 0.0631 | 0.0472 |
| R1(F),a I > 2σ(I) | 0.1474 | 0.0765 |
| wR2(F2),b all data | 0.3942 | 0.2109 |
| S(F2),c all data | 1.071 | 1.069 |

[a] $R1(F) = \Sigma||F_0|-|F_C||/\Sigma|F_0|$; [b] $wR2(F^2) = [\Sigma w(F_0^2-F_C^2)^2/\Sigma wF_0^4]^{1/2}$; [c] $S(F^2) = [\Sigma w(F_0^2-F_C^2)^2/(n+r-p)]^{1/2}$.

**Single Crystal Conductivity.** Conductivity measurements were performed on several needle-shaped single crystals of **1** in the temperature range of 300−100 K. To perform the electrical contacts, gold wires were attached directly to the crystals with silver paint. Two-probe DC measurements were performed applying a constant voltage in the range 0-2V and measuring the current using a Keithley 6487 Picoammeter/Voltage Source. Low temperature was provided by a homemade cryostat equipped with a 4 K pulse-tube.

Four-probe DC measurements were performed for compound **2** by using a diamond anvil cell (DAC). A rectangular shape of single crystal (0.17 × 0.06 × 0.03 $mm^3$) was used for ambient pressure measurement, and a size of 0.16 × 0.04 × 0.02 $mm^3$ single crystal was used for high-pressure measurements. The crystals were attached by four 5 μm gold wires with gold paint. A culet size 0.7 mm diamond anvil and Daphne Oil 7373 was used as the pressure-transmitting medium. A tension annealed stainless still (SUS301) was used as metal gasket. The pressure was determined by the shift of the ruby fluorescence R1 lines at room temperature. The Cryocooler helium compressor system (Sumitomo Heavy Industries, Ltd.) was used for cooling DAC with cooling rate of 1.5K/min. The KEITHLEY 224 Programmable current source and 182 Sensitive digital voltmeter were used for all measurements.

**Computational Details.** The tight-binding band structure calculations were of the extended Hückel type.[19] A modified Wolfsberg-Helmholtz formula was used to calculate the non-diagonal $H_{\mu\nu}$ values.[20] All valence electrons were taken into account in the calculations and the basis set consisted of Slater-type orbitals of double-ζ quality for C 2s and 2p, S 3s and 3p and of single-ζ quality for H 1s. The ionization potentials, contraction coefficients and exponents were taken from previous work.[21]

## ASSOCIATED CONTENT

The Supporting Information is available free of charge on the ACS Publications website at DOI:... Additional figures as mentioned in the text.

**Accession Codes**

CCDC 1945944–1945945 contain the supplementary crystallographic data for this paper. These data can be obtained free of charge via www.ccdc.cam.ac.uk/data_request/cif, or by emailing data_request@ccdc.cam.ac.uk, or by contacting The Cambridge Crystallographic Data Centre, 12 Union Road, Cambridge CB2 1EZ, UK; fax: +44 1223 336033.

## AUTHOR INFORMATION

**Corresponding Authors**

*M.L.M.: e-mail, mercuri@unica.it; fax: (+39)0706754474; tel, (+39)0706754456.

*N.A.: e-mail: narcis.avarvari@univ-angers.fr; fax: (+33)02 41 73 5405; tel, (+33)02 41 73 50 84.

**ORCID**

Suchithra Ashoka Sahadevan: 0000-0001-7335-9549
Alexandre Abhervé: 0000-0002-3883-310X
Joan Cano: 0000-0002-7382-7135
Francesc Lloret: 0000-0003-2959-0879
Miguel Julve: 0000-0001-9006-8268
Enric Canadell: 0000-0002-4663-5226
Maria Laura Mercuri: 0000-0002-4816-427X
Narcis Avarvari: 0000-0001-9970-4494

**Notes**

The authors declare no competing financial interest.

**ACKNOWLEDGMENTS**

This work was supported in France by the CNRS, the University of Angers, the RFI Regional LUMOMAT project ASCO-MMM (grant to A.A.). The work in Italy was supported by the Fondazione di Sardegna-Convenzione triennale tra la Fondazione di Sardegna e gli Atenei Sardi, Regione Sardegna-L.R. 7/2007 annualità 2016-DGR 28/21 del 17.05.2015 "Innovative Molecular Functional Materials for Environmental and Biomedical Applicatons" (grant to S.A.S.) and INSTM. M.J.O. acknowledges support from the Ministerio Español de Ciencia e Innovación (Project CTQ2016-75068P) and Unidad de Excelencia María de Maeztu (Project MDM-2015-0538). Work at Bellaterra (Spain) was supported by the Spanish MICIU through Grant PGC2018-096955-B-C44 and the MINECO through the Severo Ochoa Centers of Excellence Program under Grant SEV-2015-0496 as well as by Generalitat de Catalunya (2017SGR1506).

**DEDICATION**

Dedicated to Professor Marius Andruh on the occasion of his 65th anniversary.

## REFERENCES

(1) a) Kobayashi, H.; Cui, H.; Kobayashi, A. Organic Metals and Superconductors Based on BETS (BETS = Bis(ethylenedithio)tetraselenafulvalene). *Chem. Rev.* **2004**, *104*, 5265–5288. b) Enoki, T.; Miyazaki, A. Magnetic TTF-Based Charge-Transfer Complexes. *Chem. Rev.* **2004**, *104*, 5449–5478. c) Coronado, E.; Giménez-Saiz, C.; Gómez-García, C. J. Recent Advances in Polyoxometalate-Containing Molecular Conductors. *Coord. Chem. Rev.* **2005**, *249*, 1776–1796. d) Rashid, S.; Turner, S. S.; Day, P.; Howard, J. A. K.; Guionneau, P.; McInnes, E. J. L.; Mabbs, F. E.; Clark, R. J. H.; Firth, S.; Biggs, T. New Superconducting Charge-Transfer Salts $(BEDT\text{-}TTF)_4[A{\cdot}M(C_2O_4)_3]{\cdot}C_6H_5NO_2$ ($A = H_3O$ or $NH_4$, M = Cr or Fe, BEDT-TTF = Bis(Ethylenedithio)Tetrathiafulvalene). *J. Mater. Chem.* **2001**, *11*, 2095–2101. e) Martin, L.; Turner, S. S.; Day, P.; Mabbs, F. E.; McInnes, E. J. L. New Molecular Superconductor Containing Paramagnetic Chromium(III) Ions. *Chem Commun.* **1997**, *15*, 1367–1368. f) Uji, S.; Shinagawa, H.; Terashima, T.; Yakabe, T.; Terai, Y.; Tokumoto, M.; Kobayashi, A.; Tanaka, H.; Kobayashi, H. Magnetic-Field-Induced Superconductivity in a

Two-Dimensional Organic Conductor. *Nature.* **2001**, *410*, 908–910. g) Lorcy, D.; Bellec, N.; Fourmigué, M.; Avarvari, N. Tetrathiafulvalene-based group XV ligands: Synthesis, coordination chemistry and radical cation salts. *Coord. Chem. Rev.* **2009**, *253*, 1398–1438. h) Almeida M. Editorial: Magnetism of Molecular Conductors. *Magnetochemistry* **2017**, *3*, 23.

(2) Kurmoo, M.; Graham, A. W.; Day, P.; Coles, S. J.; Hursthouse, M. B.; Caulfield, J. L.; Singleton, J.; Pratt, F. L.; Hayes, W.; Ducasse, L.; Guionneau, P. Superconducting and Semiconducting Magnetic Charge Transfer Salts: (BEDT-TTF)$_4$AFe($C_2O_4$)$_3$·$C_6H_5CN$ (A = $H_2O$, K, $NH_4$) *J. Am. Chem. Soc.* **1995**, *117*, 12209–12217.

(3) a) Fujiwara, H.; Fujiwara, E.; Nakazawa, Y.; Narymbetov, B. Z.; Kato, K.; Kobayashi, H.; Kobayashi, A.; Tokumoto, M.; Cassoux, P. A Novel Antiferromagnetic Organic Superconductor κ-(BETS)$_2$FeBr$_4$ [where BETS= Bis (Ethylenedithio)Tetraselenafulvalene]. *J. Am. Chem. Soc.* **2001**, *123*, 306–314. b) Day, P.; Kurmoo, M.; Mallah, T.; Marsden, I.R.; Friend, R.H.; Pratt, F.L.; Hayes, W.; Chasseau, D.; Gaultier, J.; Bravic, J.; Ducasse, L. Structure and Properties of Tris[bis(ethylenedithio)tetrathiafulvalenium]tetrachlorocopper(II) Hydrate, (BEDT-TTF)$_3$$CuCl_4$.$H_2O$: First Evidence for Coexistence of Localized and Conduction Electrons in a Metallic Charge-Transfer Salt. *J. Am. Chem. Soc.* **1992**, *114*, 10722–10729. c) Martin, L.; Day, P.; Clegg, W.; Harrington, R.W.; Horton, P.N.; Bingham, A.; Hursthouse, M.B.; McMillan, P.; Firth, S. Multi-Layered Molecular Charge-Transfer Salts Containing Alkali Metal Ions. *J. Mater. Chem.* **2007**, *17*, 3324–3329.

(4) a) Martin, L.; Turner, S. S.; Day, P.; Guionneau, P.; Howard, J. A. K.; Hibbs, D. E.; Light, M. E.; Hursthouse, M. B.; Uruichi, M.; Yakushi, K. Crystal Chemistry and Physical Properties of Superconducting and Semiconducting Charge Transfer Salts of the Type (BEDT-TTF)$_4$[$A^IM^{III}$($C_2O_4$)$_3$]·PhCN ($A^I$ = $H_3O$, $NH_4$, K; $M^{III}$ = Cr, Fe, Co, Al; BEDT-TTF = Bis(ethylenedithio)tetrathiafulvalene) *Inorg. Chem.* **2001**, *40*, 1363–1371. b) Akutsu, H.; Akutsu-Sato, A.; Turner, S. S.; Le Pévelen, D.; Day, P.; Laukhin, V.; Klehe, A.-K.; Singleton, J.; Tocher, D. A.; Probert, M. R.; Howard, J. A. K. Effect of Included Guest Molecules on the Normal State Conductivity and Superconductivity of β‘ ‘-(ET)$_4$[($H_3O$)Ga($C_2O_4$)$_3$]·G (G = Pyridine, Nitrobenzene) *J. Am. Chem. Soc.* **2002**, *124*, 12430–12431. c) Coronado, E.; Curreli, S.; Giménez-Saiz, C.; Gómez-García, C. J. New magnetic conductors and superconductors based on BEDT-TTF and BEDS-TTF *Synth. Met.* **2005**, *154,* 245–248. d) Coronado, E.; Curreli, S.; Giménez-Saiz, C.; Gómez-García, C. J. A novel paramagnetic molecular

superconductor formed by bis(ethylenedithio)tetrathiafulvalene, tris(oxalato)ferrate(III) anions and bromobenzene as guest molecule: $ET_4[(H_3O)Fe(C_2O_4)_3]\cdot C_6H_5Br$. *J. Mater. Chem.* **2005**, *15*, 1429–1436. e) Prokhorova, T. G.; Khasanov, S. S.; Zorina, L. V.; Buravov, L. I.; Tkacheva, V. A.; Baskakov, A. A.; Morgunov, R. B.; Gener, M.; Canadell, E.; Shibaeva, R. P.; Yagubskii, E. B. Molecular Metals Based on BEDT-TTF Radical Cation Salts with Magnetic Metal Oxalates as Counterions: β"-(BEDT-TTF)$_4$A[M$(C_2O_4)_3$]·DMF (A = $NH_4^+$, $K^+$; M = $Cr^{III}$, $Fe^{III}$). *Adv. Funct. Mat.* **2003**, *13*, 403–411. f) Martin, L.; Morritt, A. L.; Lopez, J. R.; Akutsu, H.; Nakazawa, Y.; Imajo, S.; Ihara, Y. Ambient-pressure molecular superconductor with a superlattice containing layers of tris(oxalato)rhodate enantiomers and 18-crown-6. *Inorg. Chem.* **2017**, *56*, 717–720. g) Martin, L.; Morritt, A. L.; Lopez, J. R.; Nakazawa, Y.; Akutsu, H.; Imajo, S.; Ihara, Y.; Zhang, B.; Zhang, Y.; Guo, Y. Molecular conductors from bis(ethylenedithio) tetrathiafulvalene with tris(oxalato)rhodate. *Dalton Trans.* **2017**, *46*, 9542–9548. h) Martin, L.; Lopez, J. R.; Akutsu, H.; Nakazawa, Y.; Imajo, S. Bulk Kosterlitz−Thouless Type Molecular Superconductor *β″*-(BEDTTTF)$_2$[$(H_2O)(NH_4)_2Cr(C_2O_4)_3$]·18-crown-6. *Inorg. Chem.* **2017**, *56*, 14045–14052. i) Martin, L. Molecular conductors of BEDT-TTF with tris(oxalato)metallate anions. *Coord. Chem. Rev.* **2018**, *376*, 277–291. j) Morritt, A. L.; Lopez, J. R.; Blundell, T. J.; Canadell, E.; Akutsu, H.; Nakazawa, Y.; Imajo, S.; Martin, L. 2D Molecular Superconductor to Insulator Transition in the *β″*-(BEDT-TTF)$_2$[$(H_2O)(NH_4)_2M(C_2O_4)_3$]·18-crown-6 Series (M = Rh, Cr, Ru, Ir). *Inorg. Chem.* **2019**, DOI: 10.1021/acs.inorgchem.9b00292.

(5) a) Coronado, E.; Galán-Mascarós, J. R.; Gómez-García, C.; Laukhin, V. Coexistence of ferromagnetism and metallic conductivity in a molecule-based layered compound. *Nature* **2000**, *408*, 447–449. b) Clemente-Leon, M.; Coronado, E.; Martí-Gastaldo, C.; Romero, F. M. Multifunctionality in hybrid magnetic materials based on bimetallic oxalate complexes *Chem. Soc. Rev.* **2011**, *40*, 473−497.

(6) a) Atzori, M.; Marchiò, L.; Clérac, R.; Serpe, A.; Deplano, P.; Avarvari, N.; Mercuri, M. L. Hydrogen-Bonded Supramolecular Architectures Based on tris(Hydranilato)Metallate(III) (M = Fe, Cr) Metallotectons. *Cryst. Growth Des.* **2014**, *14*, 5938–5948. b) Atzori, M.; Artizzu, F.; Sessini, E.; Marchiò, L.; Loche, D.; Serpe, A.; Deplano, P.; Concas, G.; Pop, F.; Avarvari, N.; Mercuri, M. L. Halogen-Bonding in a New Family of Tris(Haloanilato)Metallate(III) Magnetic Molecular Building Blocks. *Dalton Trans.* **2014**, *43*, 7006–7019. c) Atzori, M.;

Artizzu, F.; Marchiò, L.; Loche, D.; Caneschi, A.; Serpe, A.; Deplano, P.; Avarvari, N.; Mercuri, M. L. Switching-on Luminescence in Anilate-Based Molecular Materials. *Dalton Trans.* **2015**, *44*, 15786–15802.

(7) a) Gómez-Claramunt, P.; Benmansour, S.; Hernández-Paredes, A.; Cerezo-Navarrete, C.; Rodríguez-Fernández, C.; Canet-Ferrer, J.; Cantarero, A.; Gómez-García, C. J. Tuning the Structure and Properties of Lanthanoid Coordination Polymers with an Asymmetric Anilato Ligand. *Magnetochemistry* **2018**, *4*, 6. b) Benmansour, S.; Pérez-Herráez, I.; López-Martínez, G.; Gómez-García, C. J. Solvent-Modulated Structures in Anilato-Based 2D Coordination Polymers. *Polyhedron* **2017**, *135*, 17–25. c) Sahadevan, S. A.; Monni, N.; Abhervé, A.; Marongiu, D.; Sarritzu, V.; Sestu, N.; Saba, M.; Mura, A.; Bongiovanni, G.; Cannas, C.; Quochi, F.; Avarvari, N.; Mercuri, M. L. Nanosheets of Two-Dimensional Neutral Coordination Polymers Based on Near-Infrared-Emitting Lanthanides and a Chlorocyananilate Ligand. *Chem. Mater.* **2018**, *30*, 6575–6586. d) Benmansour, S.; Hernández-Paredes, A.; Gómez-García, C. J. Two Dimensional Magnetic Coordination Polymers Formed by Lanthanoids and Chlorocyananilato. *Magnetochemistry*, **2018**, *4*, 58-73.

(8) a) Atzori, M.; Benmansour, S.; Mínguez Espallargas, G.; Clemente-León, M.; Abhervé, A.; Gómez-Claramunt, P.; Coronado, E.; Artizzu, F.; Sessini, E.; Deplano, P.; Serpe, A.; Mercuri, M. L.; Gómez-García, C. J. A Family of Layered Chiral Porous Magnets Exhibiting Tunable Ordering Temperatures. *Inorg. Chem.* **2013**, *52*, 10031–10040. b) Benmansour, S.; Vallés-García, C.; Gómez-Claramunt, P.; Mínguez Espallargas, G.; Gómez-García, C. J. 2D and 3D Anilato-Based Heterometallic M(I)M(III) Lattices: The Missing Link. *Inorg. Chem.* **2015**, *54*, 5410–5418

(9) a) Atzori, M.; Pop, F.; Auban-Senzier, P.; Gómez-García, C. J.; Canadell, E.; Artizzu, F.; Serpe, A.; Deplano, P.; Avarvari, N.; Mercuri, M. L. Structural Diversity and Physical Properties of Paramagnetic Molecular Conductors Based on Bis(Ethylenedithio)Tetrathiafulvalene (BEDT-TTF) and the Tris(Chloranilato)Ferrate(III) Complex. *Inorg. Chem.* **2014**, *53*, 7028–7039. b) Benmansour, S.; Abhervé, A.; Gómez-Claramunt, P.; Vallés-García, C.; Gómez-García, C. J. Nanosheets of Two-Dimensional Magnetic and Conducting Fe(II)/Fe(III) Mixed-Valence Metal-Organic Frameworks. *ACS Appl. Mater. Interfaces* **2017**, *9*, 26210–26218. c) Sahadevan, S. A.; Abhervé, A.; Monni, N.; Sáenz de Pipaón, C.; Galán-Mascarós, J. R.; Waerenborgh, J. C.; Vieira, B. J. C.; Auban-

Senzier, P.; Pillet, S.; Bendeif, E.-E.; Alemany, P.; Canadell, E.; Mercuri, M. L.; Avarvari, N. Conducting Anilate-Based Mixed-Valence Fe(II)Fe(III) Coordination Polymer: Small-Polaron Hopping Model for Oxalate-Type Fe(II)Fe(III) 2D Networks. *J. Am. Chem. Soc.* **2018**, *140*, 12611–12621. d) Benmansour, S.; Coronado, E.; Giménez-Saiz, C.; Gómez-García, C. J.; Rößer, C. Metallic Charge-Transfer Salts of Bis(Ethylenedithio)Tetrathiafulvalene with Paramagnetic Tetrachloro(Oxalato)Rhenate(IV) and Tris(Chloranilato)Ferrate(III) Anions. *Eur. J. Inorg. Chem.* **2014**, *2014*, 3949–3959.

(10) a) Abhervé, A.; Clemente-León, M.; Coronado, E.; Gómez-García, C. J.; Verneret, M. One-Dimensional and Two-Dimensional Anilate-Based Magnets with Inserted Spin-Crossover Complexes. *Inorg. Chem.* **2014**, *53*, 12014–12026. b) Mercuri, M. L.; Congiu, F.; Concas, G.; Sahadevan, S. A. Recent Advances on Anilato-Based Molecular Materials with Magnetic and/or Conducting Properties. *Magnetochemistry* **2017**, *3*, 17-73. c) Sahadevan, S. A.; Monni, N.; Abhervé, A.; Auban-Senzier, P.; Canadell, E.; Mercuri, M. L.; Avarvari, N. Synthesis and Physical Properties of Purely Organic BEDT-TTF-Based Conductors Containing Hetero-/Homosubstituted Cl/CN-Anilate Derivatives. *Inorg. Chem.* **2017**, *56*, 12564–12571. d) Sahadevan, S. A.; Monni, N.; Abhervé, A.; Cosquer, G.; Oggianu, M.; Ennas, G.; Yamashita, M.; Avarvari, N.; Mercuri, M. L. Dysprosium Chlorocyanoanilate-Based 2D-Layered Coordination Polymers. *Inorg. Chem.* **2019**, DOI: 10.1021/acs.inorgchem.9b01968.

(11) a) Pop, F.; Laroussi, S.; Cauchy, T.; Gómez-García, C. J.; Wallis, J. D.; Avarvari, N. Tetramethyl-Bis(ethylenedithio)-Tetrathiafulvalene (TM-BEDT-TTF) Revisited: Crystal Structures, Chiroptical Properties, Theoretical Calculations and a Complete Series of Conducting Radical Cation Salts. *Chirality* **2013**, *25*, 466–474. b) Yang, S.; Pop, F.; Melan, C.; Brooks, A. C.; Martin, L.; Horton, P.; Auban-Senzier, P.; Rikken, G. L. J. A..; Avarvari, N.; Wallis, J. D. Charge transfer complexes and radical cation salts of chiral methylated organosulfur donors. *CrystEngComm.* **2014**, *16*, 3906–3916.

(12) Atzori, M.; Pop, F.; Auban-Senzier, P.; Clérac, R.; Canadell, E.; Mercuri, M. L.; Avarvari, N. Complete Series of Chiral Paramagnetic Molecular Conductors Based on Tetramethyl-Bis(Ethylenedithio)-Tetrathiafulvalene (TM-BEDT-TTF) and Chloranilate-Bridged Heterobimetallic Honeycomb Layers. *Inorg. Chem.* **2015**, *54*, 3643–3653.

(13) Guionneau, P.; Kepert, C. J.; Bravic, G.; Chasseau, D.; Truter, M. R.; Kurmoo, M.; Day, P. Determining the Charge Distribution in BEDT-TTF Salts. *Synth. Met.* **1997**, *86*, 1973–1974.

(14) Williams, J. M.; Ferraro, J. R.; Thorn, R. J.; Carlson, K. D.; Geiser, U.; Wang, H. H.; Kini, A. M.; Whangbo, M. H. in "*Organic Superconductor: Synthesis, Structure, Properties and Theory*", ed. R. N. Crimes, Prentice Hall, Englewood Ciffs, NJ, **1992**.

(15) a) Gómez-García, C. J.; Coronado, E.; Curreli, S.; Giménez-Saiz, C.; Deplano, P.; Mercuri, M. L.; Pilia, L.; Serpe, A.; Faulmann, C.; Canadell, E. A Chirality-Induced Alpha Phase and a Novel Molecular Magnetic Metal in the BEDT-TTF/Tris(Croconate)Ferrate(III) Hybrid Molecular System. *Chem. Commun.* **2006**, *0*, 4931–4933. b) Mercuri, M. L.; Deplano, P.; Serpe, A.; Artizzu F. *Multifunctional Materials of Interest in Molecular Electronics.* In *Handbook of Multifunctional Molecular Materials*; L. Ouahab, Ed.; Pan Stanford Publishing: Singapore, **2013**, 219 (ISBN: 9789814364249); c) Coronado, E.; Curreli, S.; Giménez-Saiz, C.; Gómez-García, C. J.; Deplano, P.; Mercuri, M. L.; Serpe, A.; Pilia, L.; Faulmann, C.; Canadell, E. New BEDT-TTF/$[Fe(C_5O_5)_3]^{3-}$ Hybrid System: Synthesis, Crystal Structure, and Physical Properties of a Chirality-Induced α Phase and a Novel Magnetic Molecular Metal *Inorg. Chem.* **2007**, *46*, 4446–4457.

(16) Pilia, L.; Sessini, E.; Artizzu, F.; Yamashita, M.; Serpe, A.; Kubo, K.; Ito, H.; Tanaka, H.; Kuroda, S.; Yamada, J.; Deplano, P.; Gómez-García, C. J.; Mercuri, M. L. New BDH-TTP/$[M^{III}(C_5O_5)_3]^{3-}$ (M = Fe, Ga) Isostructural Molecular Metals. *Inorg. Chem.* **2013**, *52*, 423–430.

(17) Graham, A. W.; Kurmoo, M.; Day, P. β″-(bedt-ttf)$_4$[$(H_2O)Fe(C_2O_4)_3$]·PhCN: the first molecular superconductor containing paramagnetic metal ions *J. Chem. Soc.*, *Chem Commun.* **1995**, *0*, 2061–2062.

(18) a) Pop, F.; Auban-Senzier, P.; Canadell, E.; Rikken, G. L. J. A.; Avarvari, N. Electrical magneto-chiral anisotropy in a bulk chiral molecular conductor. *Nat. Commun.* **2014**, *5*, 3757. b) Pop, F.; Zigon, N.; Avarvari, N. Main-Group-Based Electro- and Photoactive Chiral Materials. *Chem. Rev.* **2019**, *119*, 8435–8478.

(19) Whangbo, M.-H.; Hoffmann, R. The band structure of the tetracyanoplatinate chain. *J. Am. Chem. Soc* **1978**, *100*, 6093–6098.

(20) Ammeter, J. H.; Bürgi, H.-B.; Thibeault, J.; Hoffmann, R. Counterintuitive orbital mixing in semiempirical and ab initio molecular orbital calculations. *J. Am. Chem. Soc*. **1978**, *100*, 3686–3692.

(21) Pénicaud, A.; Boubekeur, K.; Batail, P.; Canadell, E.; Auban-Senzier, P.; Jérome, D.

Hydrogen-Bond Tuning of Macroscopic Transport Properties from the Neutral Molecular Component Site along the Series of Metallic Organic-Inorganic Solvates (BEDT-TTF)$_4$Re$_6$Se$_5$C1$_9$·[guest], [guest = DMF, THF, dioxane]. *J. Am. Chem. Soc.* **1993**, *115*, 4101–4112.

## Table of Contents Entry

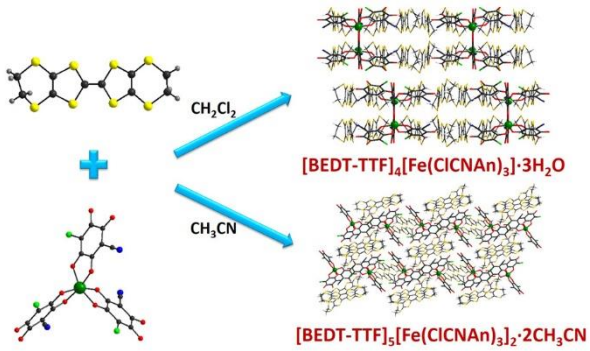


Electrocrystallization in different conditions provided two conducting crystalline BEDT-TTF radical cation salts with the paramagnetic iron(III) chlorocyanoanilate anionic complex.